Synthesis, Biological Evaluation, and Molecular Modeling Investigation of New Chiral Fibrates with PPARα and PPARγ Agonist Activity

ARTICLE *in* JOURNAL OF MEDICINAL CHEMISTRY · SEPTEMBER 2005

Impact Factor: 5.45 · DOI: 10.1021/jm0502844 · Source: PubMed

12 AUTHORS, INCLUDING:

Antonio Laghezza
Università degli Studi di Bari Aldo Moro
45 PUBLICATIONS **415** CITATIONS
SEE PROFILE

Giuseppe Fracchiolla
Università degli Studi di Bari Aldo Moro
52 PUBLICATIONS **665** CITATIONS
SEE PROFILE

Antonio Lavecchia
University of Naples Federico II
118 PUBLICATIONS **2,412** CITATIONS
SEE PROFILE

Ettore Novellino
University of Naples Federico II
610 PUBLICATIONS **8,809** CITATIONS
SEE PROFILE

Synthesis, Biological Evaluation, and Molecular Modeling Investigation of New Chiral Fibrates with PPARα and PPARγ Agonist Activity

Alessandra Pinelli,[†] Cristina Godio,[†] Antonio Laghezza,[‡] Nico Mitro,[†] Giuseppe Fracchiolla,[‡] Vincenzo Tortorella,[‡] Antonio Lavecchia,[§] Ettore Novellino,[§] Jean-Charles Fruchart,[||] Bart Staels,[||] Maurizio Crestani,[†] and Fulvio Loiodice*[,‡]

Dipartimento di Scienze Farmacologiche, Università degli Studi di Milano, via Balzaretti 9, 20133 Milano, Italia, Dipartimento Farmaco-Chimico, Università degli Studi di Bari, via Orabona 4, 70126 Bari, Italia, Dipartimento di Chimica Farmaceutica, Università degli Studi di Napoli, via Montesano 49, 80131 Napoli, Italia, and U545 Inserm, Departement d'Atherosclerose, Institut Pasteur de Lille and Faculté de Pharmacie, Université de Lille 2, 1 rue du Prof Calmette, Lille Cedex 59019, France

Received March 30, 2005

Peroxisome proliferator-activated receptors (PPARs) are ligand-activated transcription factors that govern lipid and glucose homeostasis playing a central role in cardiovascular diseases, obesity, and diabetes. Medications targeted to PPARs have been established to treat hyperlipidemia (fibrates) and insulin resistance (glitazones). Thus, there is significant interest in developing new and specific ligands for these receptors. Here, we present the results of the screening of new ligands of PPARα and PPARγ. Optical isomers of new chiral fibrates were synthesized and tested in cell-based assays. Compound (*S*)-**7** showed a dual PPARα/γ activity, and its stereochemistry was crucial in receptor activation. Protease protection experiments suggested that this compound binds directly to PPAR. Moreover, computational studies showed that it properly docks to PPARα and γ ligand binding pockets. Interestingly, (*S*)-**7** exhibited only a modest capacity to induce the differentiation of murine fibroblasts 3T3-L1 into adipocytes compared to rosiglitazone, a well-known PPARγ agonist.

Introduction

Type 2 diabetes, previously referred to as non-insulin-dependent diabetes mellitus (NIDDM), accounts for over 90% of the diabetic cases reported in the western world. This metabolic disease, which is characterized by progressive insulin secretory dysfunction and insulin resistance at major target tissues such as skeletal muscle, liver, and adipose tissue,[1−8] is also linked to a wide spectrum of other pathophysiologic conditions including dyslipidemia (hypertriglyceridemia, decreased serum HDL cholesterol, increased small dense LDL particles), hypertension, hyperuricemia, increased plasminogen activator inhibitor-1 (PAI-1), abnormal fibrinolytic system, and abdominal obesity.[9,10] Several drugs are currently available for the treatment of type 2 diabetes including various insulin formulations, sulfonylureas, biguanides, and α-glucosidase inhibitors. Among the many approaches being evaluated for the discovery of new agents,[10,11] one of the most promising is certainly represented by the exploitation of peroxisome proliferator-activated receptor (PPAR) ligands. The PPARs were cloned a decade ago as orphan members of the superfamily of nuclear transcription factors that includes the receptors for steroid, retinoid, and thyroid hormones.[12] There are three PPAR subtypes which are the products of distinct genes and are commonly designated PPARα, PPARγ, and PPARβ/δ. The PPARs heterodimerize with another nuclear receptor, the 9-*cis*-retinoic acid receptor (RXR),[13,14] forming a complex that interacts with specific DNA response elements within promoter regions of target genes. When activated by agonist ligand binding, this heterodimer complex recruits transcription coactivators and regulates the transcription of genes involved in the control of lipid and carbohydrate metabolism.

Fibrates are a class of drugs that reduce serum triglycerides and increase HDL cholesterol through activation of PPARα which is expressed predominantly in the liver.[15] This receptor activation has also been shown to produce antiinflammatory effects in vascular cells with possible beneficial effects in the prevention of atherosclerosis.[16] Thiazolidine-2,4-diones (TZDs or glitazones), on the other hand, are antidiabetic agents that improve the blood glucose level in type 2 diabetes by an insulin-sensitizing mechanism related to a selective activation of PPARγ subtype.[17] Compounds with dual PPARα/PPARγ activity, thus, appear well-suited for the treatment of diabetic patients with the additional risk factor of dyslipidemia. So far, therefore, a relatively high number of dual PPARα and PPARγ agonists have been described.[18−29]

Recently,[30] we reported the effects on PPARα of some chiral analogues **2** of clofibric acid **1** (Figure 1), the active metabolite of the hypolipidemic drug clofibrate.

The potency of these compounds in activating the receptor was increased by the presence of a methylene group between the aromatic ring and the phenolic oxygen and by the enlargement of the aromatic moiety to a biphenyl group. On the other hand, a more extensive aromatic portion is present, also, in the series of new aryloxyacetic acids[31,32] **3** with dual PPARα/

* To whom correspondence should be addressed. Phone: +39 080-5442798. Fax: +39 080-5442231. E-mail: floiodice@farmchim.uniba.it.
[†] Università degli Studi di Milano.
[‡] Università degli Studi di Bari.
[§] Università degli Studi di Napoli.
[||] Université de Lille 2.

10.1021/jm0502844 CCC: $30.25
Published on Web 08/04/2005

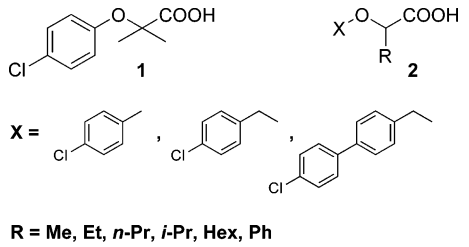

Figure 1. Clofibric acid and chiral analogues.

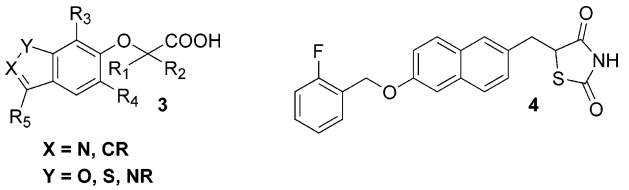

Figure 2. Dual PPARα/PPARγ agonists.

PPARγ activity as well as in netoglitazone **4**, a thiazolidinedione PPARα/PPARγ agonist established as an antidiabetic drug in animal models of Type 2 diabetes (Figure 2).[33,34] Moreover, these analogues **2** displayed a high degree of stereoselectivity when either a phenyl or an *n*-propyl group was located in α to the carboxylic function; in fact, the (*S*)-isomers were much more active than the (*R*)-isomers. Afterward, another example of stereoselectivity was reported in a patent for the chiral clofibric acid analogue halofenate, whose levo-isomer was shown to significantly reduce plasma glucose differently from the dextro-isomer.[35] For this enantiomer, described only very recently as a selective PPAR modulator, a Phase 2 trial was started with the name of metaglidasen.[36]

The combination of these structural elements led us to the formulation of the new chiral clofibric acid analogues **5** and **6** (Figure 3) in which the aromatic moiety is represented by a naphthyl and a 4-(4-chlorophenyl)benzyl group, respectively, and the substituent on the stereogenic center by an *n*-propyl alkyl chain.

Additionally, compound **7** (Figure 3) was investigated as representative of the structural simplification of β-aryl-α-oxysubstituted propanoic acids for which recent reports have suggested very potent in vitro and in vivo PPARα and PPARγ activities.[20,21,28,29,37] The development of molecules with reduced molecular weight, in fact, does not necessarily provide weak PPAR agonists[32,38,39] and, on the other hand, improves pharmacokinetic and pharmaceutic properties.[39]

Compounds **5**−**7** were synthesized in optically active form and both (*R*)- and (*S*)-isomers were evaluated for their PPARα/PPARγ activity by the transactivation assay, a powerful and widely used assay whose good correlation with in vivo activity is generally accepted.

Only the enantiomer (*S*)-**7** showed an interesting dual agonist activity and this prompted us to investigate other analogues of this series (**8**−**15**, Figure 3) in which the influence of different substituents on the phenolic ring was examined. According to the results obtained with compound **7**, all of these analogues were synthesized only as the (*S*)-isomers.

Chemistry. Both enantiomers of compounds **5** and **6** were obtained starting from the optical isomers of 2-hydroxypentanoic acid readily prepared from commercially available (L)- and (D)-norvaline.[40] Synthesis

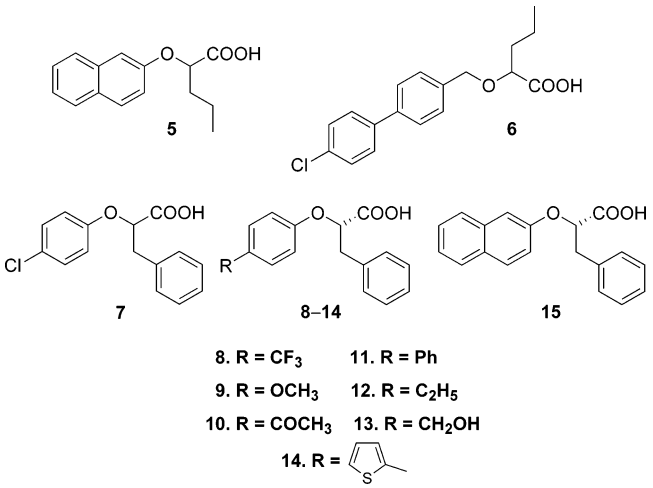

Figure 3. New chiral clofibric acid analogues.

Scheme 1[a]

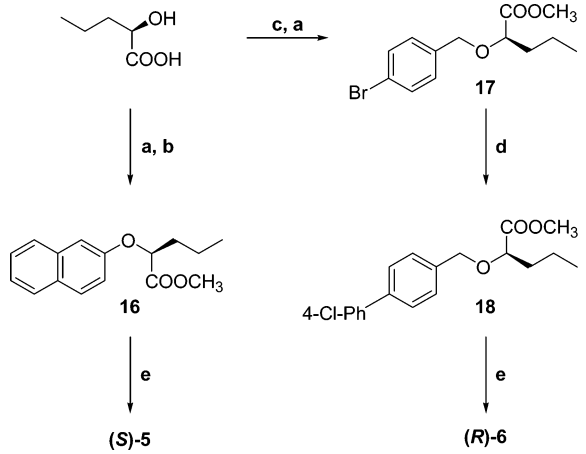

[a] (a) CH_2N_2, Et_2O; (b) 2-naphthol, PPh_3, DEAD, THF, rt; (c) NaH 95%, 4-$BrC_6H_4CH_2Br$, DMF, rt; (d) $Pd(PPh_3)_4$, K_2CO_3, 4-ClC_6H_4-$B(OH)_2$, toluene, 80 °C; (e) THF, 1 N NaOH (1:1).

of compound (*S*)-**5** is depicted in Scheme 1 and involved the esterification of (*R*)-2-hydroxypentanoic acid with diazomethane and the condensation with 2-naphthol under Mitsunobu conditions followed by saponification to the desired acid. On the other hand, the reaction of (*R*)-2-hydroxypentanoic acid with 4-bromobenzyl bromide and subsequent esterification with diazomethane led to the intermediate bromobenzyl ether **17** whose Suzuki cross-coupling reaction with 4-chlorophenylboronic acid, followed by saponification with NaOH in THF/H_2O, provided compound (*R*)-**6** (Scheme 1).

The synthesis of the isomers (*R*)-**5** and (*S*)-**6** was carried out in identical fashion starting from (*S*)-2-hydroxypentanoic acid. Analogues (*S*)-**7**, **8**−**12**, and **15** were prepared via a Mitsunobu reaction of the suitable 4-substituted phenol or 2-naphthol with (*R*)-methyl (or ethyl) phenyllactate, followed by saponification of the so obtained products **19b**−**h** to the desired acids (Scheme 2). In the same way the isomer (*R*)-**7** was obtained starting from (*S*)-methyl phenyllactate. For compounds **13** and **14**, the Mitsunobu reaction of 4-bromophenol or 4-hydroxybenzaldehyde with (*R*)-methyl (or ethyl) phenyllactate yielded **19i** and **19a**, respectively; the former was reduced with $NaBH_4$, the latter was condensed with 2-thiopheneboronic acid under Suzuki conditions. The subsequent saponification of the inter-

Scheme 2[a]

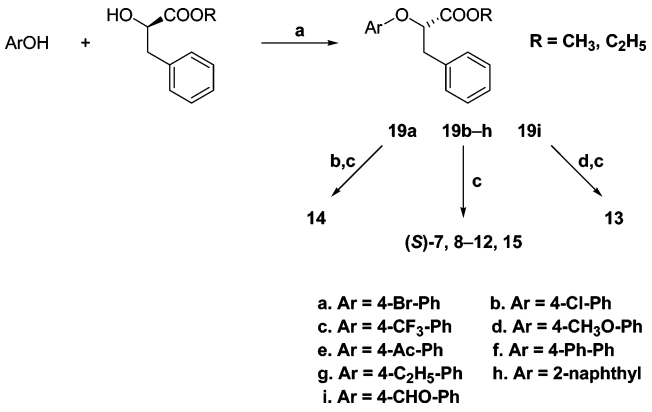

[a] (a) PPh_3, DIAD, toluene, rt; (b) $Pd(PPh_3)_4$, K_2CO_3, 2-thiopheneboronic acid, toluene, 80 °C; (c) THF, 1 N NaOH (1:1); (d) $NaBH_4$, THF/H_2O (1:1), 0 °C.

mediate esters so obtained led to the target compounds (Scheme 2).

All of the final optically active acids **5**−**15** had enantiomeric excesses >98% as determined by HPLC analysis on chiral stationary phase (see Experimental Section).

Results and Discussion

Compounds **5**−**15**, as well as clofibric acid, were evaluated for their agonist activity on the human PPARα (hPPARα) and PPARγ (hPPARγ) subtypes. For this purpose, GAL4-PPAR chimeric receptors were expressed in transiently transfected HepG2 cells according to a previously reported procedure.[41] The results obtained (Table 1) were compared with corresponding data for Wy-14,643 and rosiglitazone used as reference compounds in the PPARα and PPARγ transactivation assays, respectively. Maximum obtained fold induction with the reference agonist was defined as 100%.

The enantiomers of compounds **5**−**7** were examined first (Table 1). (*R*)-**6** and (*S*)-**6** displayed a weak activity on PPARα and a negligible activation of PPARγ, but the substitution of the chloro-biphenylmethylene system in **6** with the much more planar naphthalene ring gave **5** whose enantiomers behaved differently. (*S*)-**5**, in fact, was a more potent and selective PPARα agonist than clofibric acid and almost as efficacious as Wy-14,643, although less potent, whereas (*R*)-**5** was virtually ineffective on both receptor subtypes. However, the removal of the phenylmethylene moiety in **6** as well as the replacement of the *n*-propyl group on the stereogenic center with benzyl afforded **7** which exhibited the most interesting profile. Its (*S*)-enantiomer displayed a remarkable dual PPARα/PPARγ activity; its efficacy on PPARα was higher than that of clofibric acid and comparable to that of Wy-14,643 with the potency about half of the reference compound. In addition, (*S*)-**7** was much more active than clofibric acid in activating PPARγ, although not as potent and effective as rosiglitazone. The stereochemistry still played a crucial role being the (*R*)-enantiomer virtually ineffective on both PPAR isoforms.

According to the results obtained with compound **7**, its analogues **8**−**15**, in which the influence of different substituents on the phenolic ring was examined, were prepared only as the (*S*)-isomers. The substituents introduced in place of the chlorine in **7** affected both PPARα and PPARγ agonist activity almost with the same rank order (Table 1). The introduction of the strong electron-withdrawing trifluoromethyl group provided compound **8** with increased PPARα and γ potency, but slightly lower efficacy toward both receptor isotypes. However, the introduction of the acetyl group with similar electronic characteristics, but poor lipophilicity, afforded compound **10** with less agonist activity on both PPARα and PPARγ. Similar results were obtained with **9** in which the presence of the electron-donating methoxy group reduced the PPARγ activity, particularly.

A new significant improvement in both potency and efficacy was obtained with the more lipophilic aromatic rings as substituents. These compounds (**11**, **14**, **15**) were full PPARα agonists, at least as potent as Wy-14,-643, and displayed also a remarkable activity on PPARγ (Table 1). In particular, compound **11** showed the most interesting dual activity profile being also a full PPARγ agonist only approximately 10 times less potent than rosiglitazone. Similar results were obtained, also, with the introduction of a short alkyl group on the phenolic ring (compound **12**), although with a reduced potency on PPARγ. On the contrary, the substitution of the ethyl chain of **12** with a polar and hydrogen bond forming hydroxymethyl group (compound **13**) dropped the PPARα activity and produced a very weak activation of PPARγ. To ascertain the presence of the known possible species-specific selectivity of PPARα ligands,[29] the more interesting compounds of the series ((*S*)-**7**, **8**, **11**, **12**, **14**), together with clofibric acid, were also tested in the murine PPARα (mPPARα) transactivation assay. All the compounds, except clofibric acid, exhibited an increased potency particularly notable in the thiophene derivative (**14**) which was 6 times more potent on mPPARα than on hPPARα, although less efficacious (Table 1).

The same compounds were also tested with the PPARβ/δ subtype but in this case no activation was observed (data not shown), suggesting that these molecules are PPARα/γ selective ligands.

At this point, we selected compound (*S*)-**7** and tested its ability to promote differentiation of murine fibroblast 3T3-L1 cells to adipocytes, a process in which PPARγ receptors play a major role.[42,43] At the concentration of 25 μM, (*S*)-**7** was capable of inducing lipid accumulation although with less efficacy than rosiglitazone as judged by the different morphology of cells exposed to rosiglitazone and (*S*)-**7**, respectively (Figure 4). As expected, treatment of 3T3-L1 cells with (*R*)-**7** and Wy-14,643 did not result in any morphological modification (Figure 4).

To further investigate the characteristics of (*S*)-**7**, we performed the protease protection assay, a practical technique used to assess the capacity of a ligand to bind to a receptor and consequently to alter its conformation. This conformational change is reflected by the increased resistance of the receptor LBD to partial digestion by proteases.[44,45]

As shown in Figure 5, a typical protease protection pattern was obtained when hPPARγ was incubated with (*S*)-**7**. In fact, incubation of the receptor with increasing concentrations of protease (trypsin or proteinase K) in the absence of ligand leads to the complete digestion of the receptor. In contrast, when PPARγ was preincubated with (*S*)-**7** or with the thiazolidinedione ligand

Table 1. Activity of the Tested Compounds in Cell-Based Transactivation Assay[a]

	hPPARα		hPPARγ		mPPARα	
compound	EC_{50} (μM)	efficacy	EC_{50} (μM)	efficacy	EC_{50} (μM)	efficacy
R-**5**	3.9 ± 0.87	10.5 ± 1.62	12.5 ± 2.49	4.5 ± 1.04	–	–
S-**5**	8.4 ± 0.5	95.6 ± 8.75	7.2 ± 1.5	7.8 ± 1.3	–	–
R-**6**	4.0 ± 0.12	36.6 ± 5.09	5.4 ± 1.04	10.6 ± 2.77	–	–
S-**6**	3.9 ± 0.69	29.8 ± 3.12	8.9 ± 1.85	11.5 ± 1.85	–	–
R-**7**	10.9 ± 1.85	14.3 ± 1.85	10.5 ± 2.43	8 ± 1.68	–	–
S-**7**	3.9 ± 0.01	99.4 ± 12.4	2.7 ± 0.18	58.8 ± 6.01	1.3 ± 0.23	49.1 ± 7.8
8	0.5 ± 0.12	80.7 ± 11.3	0.9 ± 0.16	47.1 ± 7.11	0.27 ± 0.05	106.9 ± 12.3
9	2.5 ± 0.08	80.7 ± 9.77	20.1 ± 1.76	47.1 ± 4.28	–	–
10	13.5 ± 2.19	68.3 ± 7.17	12.4 ± 0.54	18.8 ± 3.12	–	–
11	0.5 ± 0.04	124.2 ± 10.9	0.5 ± 0.08	91.8 ± 9.02	0.2 ± 0.07	99.3 ± 10.23
12	0.7 ± 0.06	113.8 ± 1.45	3.6 ± 0.52	116 ± 14.6	0.35 ± 0.03	127.4 ± 3.29
13	28.7 ± 2.91	38.2 ± 7.51	25.7 ± 3.64	9.7 ± 1.34	–	–
14	0.9 ± 0.14	93.2 ± 8.5	1.6 ± 0.29	61.2 ± 11.96	0.15 ± 0.03	70.7 ± 10.1
15	1.4 ± 0.05	130.4 ± 13	1.5 ± 0.09	42.4 ± 8.6	–	–
clofibric acid	39.6 ± 4.1	89.7 ± 12.2	309 ± 87.3	31 ± 1.73	42 ± 6.4	67.2 ± 13.53
Wy-14,643	1.6 ± 0.3	100 ± 9.71	i.a.	i.a.	0.04 ± 0.01	100 ± 5.61
rosiglitazone	i.a.	i.a.	0.039 ± 0.003	100 ± 9.06	–	–

[a] i.a. = inactive at the tested concentrations. Values are mean ± SEM. Efficacy values were calculated as percentage of the reference compounds (Wy-14,643 for PPARα; rosiglitazone for PPARγ).

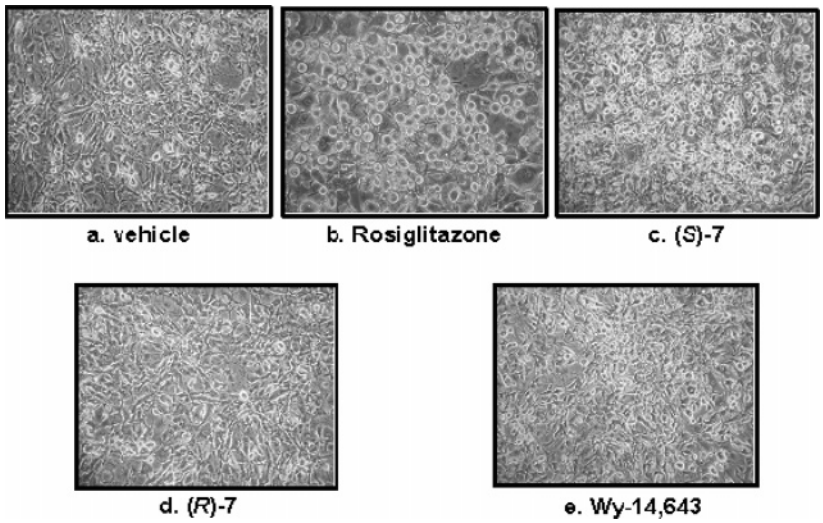

Figure 4. Effect of rosiglitazone and (*S*)-**7** on differentiation of 3T3-L1 cells. After reaching confluence, cells were stimulated with 1 μM dexamethasone, 1 μM IBMX, and 2 μM insulin for 2 days. Then the DEX/MIX medium was removed and cells were treated for 10 days with the following ligands: a. vehicle; b. 0.1 μM rosiglitazone; c. 25 μM (*S*)-**7**; d. 25 μM (*R*)-**7**; e. 25 μM Wy-14,643.

rosiglitazone, a major protease-resistant fragment of 27kDa was observed. This presumably is the result of a conformational change leading to the activation of the receptor. These results confirm that (*S*)-**7** binds directly to the PPARγ LBD and induces a conformational change in PPARγ.

To better understand the activity of the most interesting compounds (*S*)-**7** and **11** at a molecular level, docking experiments were performed into the binding pockets of the hPPARα and γ receptors[21,46] making use of the automated docking program AutoDock.[47] As a preliminary test of the docking method, GW409544, a potent full agonist on both PPARα and PPARγ,[46] was docked into the PPARα crystal structure. The docking test indicated that the cluster of similar conformations with the lowest energy docked structure reproduced very closely the crystallographic binding mode of GW409544 to PPARα.[46] The hydrogen bond network predicted by the AutoDock program was virtually identical to that found in the crystal structure. This docking test provided validation for using this program to perform docking studies of our ligands to PPARs.

Docking of (*S*)-**7** and **11** into the hPPARα revealed a consistent set of recurring binding modes. For the two investigated ligands, well-clustered docking results could be obtained. As shown in Table 2, the 50 independent docking runs carried out for each ligand generally converged to a small number of different positions ("clusters" of results differing by less than 1.5 Å rmsd). Generally, the top clusters (i.e. those with the most favorable ΔG_{bind}) were also associated with the highest frequency of occurrence, which suggests a good convergence behavior of the search algorithm. The best results in terms of free energy of binding were all located in a similar position at the active site. The most important interactions are summarized in Table 2, and a graphical representation of the binding modes is given in Figure 6.

In the most frequently occurring and most favorable result (−10.6 kcal/mol, found 28 times out of 50), the (*S*)-enantiomer of **7** is found in the center of the active site (Figure 6A), in the same orientation of the experimentally determined PPARα-bound conformation of GW409544. A binding mode very similar was also found

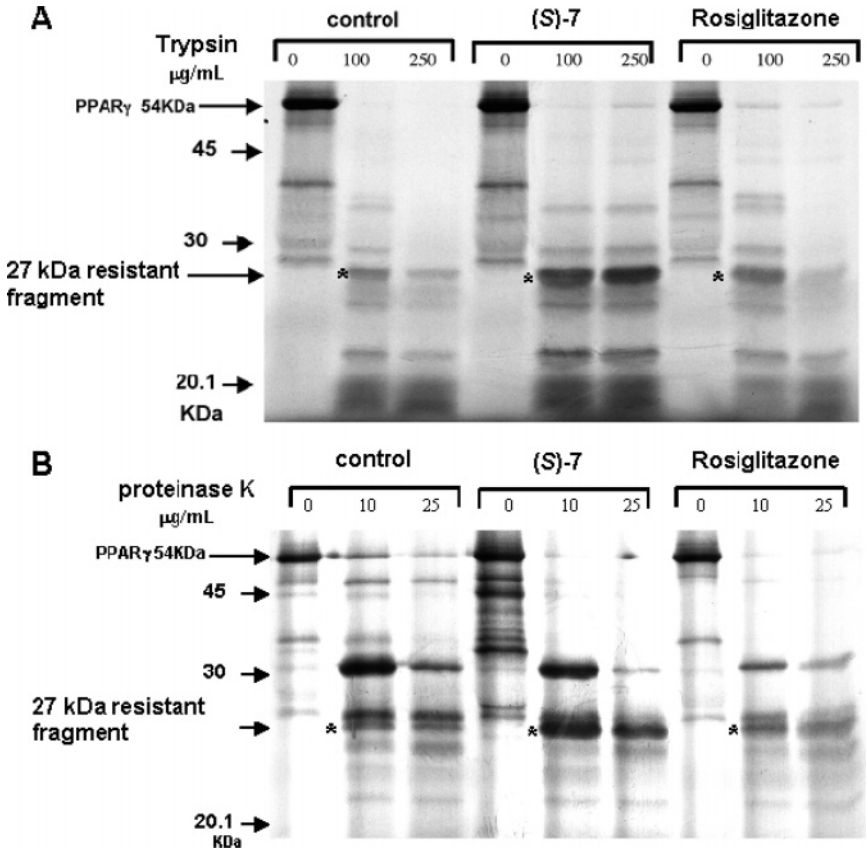

Figure 5. (*S*)-**7** induces an agonist-like conformational change in PPARγ. ^{35}S-GAL4-PPARγ LBD was synthesized in vitro and was subsequently preincubated with ethanol (control) or 25 μM (*S*)-**7** or 1 μM rosiglitazone, then incubated with distilled water or increasing concentration of trypsin (panel A) or proteinase K (panel B). Digestion products were analyzed by SDS−PAGE followed by autoradiography. An asterisk indicates the 27 kDa protease-resistant fragment of hPPARγ.

Table 2. Results of 50 Independent Docking Runs for Ligands (*S*)-**7** and **11**[a]

ligand	N_{tot}	f_{occ}	ΔG_{bind}	surrounding residues
				PPARα
(*S*)-**7**	10	28	−10.6	Phe273, Cys276, Thr279, **Ser280**, **Tyr314**, Ile317, Phe318, Leu321, Met325, Met330, Ile354, Phe351, Met355, **Tyr464**
11	12	17	−11.0	Ile272, Phe273, Cys276, Thr279, **Ser280**, **Tyr314**, Phe318, Leu321, Met330, Met335, Leu344, Leu347, Phe351, Ile354, **Tyr464**
				PPARγ
(*S*)-**7**	12	36	−8.5	Phe282, Cys285, **Ser289**, Arg288, His323, Tyr327, Leu330, Met334, Phe363, Met364, **Tyr473**, His449
11	27	10	−10.3	Ile281, Phe282, Cys285, **Ser289**, Arg288, His323, **Tyr327**, Leu330, Met334, Leu353, Leu356, Phe360, Phe363, Met364, **Tyr473**, **His449**

[a] N_{tot} is the total number of clusters; the number of results in the top cluster is given by the frequency of occurrence, f_{occ}; ΔG_{bind} is the estimated free energy of binding for the top cluster results and is given in kcal/mol. The last column shows the contacting residues for the binding mode of the top cluster. Only residues with at least five van der Waals contacts to the ligand are shown. Residues that form hydrogen bonds with the ligand are highlighted in bold.

for compound **11** (Figure 6B) with a ΔG of −11.0 kcal/mol (found 17 times out of 50).

The ligands adopt a U-shaped conformation that allows the carboxylate group to form hydrogen bonds with Tyr314, Tyr464, and Ser280. The His440 N$^{\epsilon}$2 is hydrogen bonded to Tyr464 O$^{\eta}$, contributing to stabilize the hydrogen bonding network. This hydrogen bonding pattern is expected to be essential for the formation of a tight binding ligand complex which stabilizes a charge clamp[48] between the C-terminal activation function 2 (AF-2) helix and a conserved lysine residue on the surface of the receptor. The benzyl group of both (*S*)-**7** and **11** is bound into a hydrophobic cavity formed by Thr279, Ile317, Phe318, Leu321, Met325, and Met330 side chains. The Phe318 aromatic ring appears in a suitable orientation for a T-shaped interaction with the phenyl of both ligands. It is worth noting that the Cys276 side chain is in close contact with both aromatic rings of the ligand, making additional hydrophobic interactions.

The 4-chlorophenoxy ring of (*S*)-**7** points to a large hydrophobic cleft lined by residues Ile354, Met355, Phe351, and Phe273. Particularly, the electron-rich benzene ring of Phe273 appears to be optimally oriented for a favorable π-stacking interaction with the electron-deficient 4-chlorobenzene ring of the ligand: the planes of the two aromatic rings are fairly parallel and separated by a distance of 5.3 Å. As shown in Figure 6B, this hydrophobic cleft appears sufficiently large to accommodate the biphenyl group of **11**, making extensive hydrophobic contacts with the residues Ile272, Phe273, Leu344, Leu347, Phe351, Ile354, and Met355.

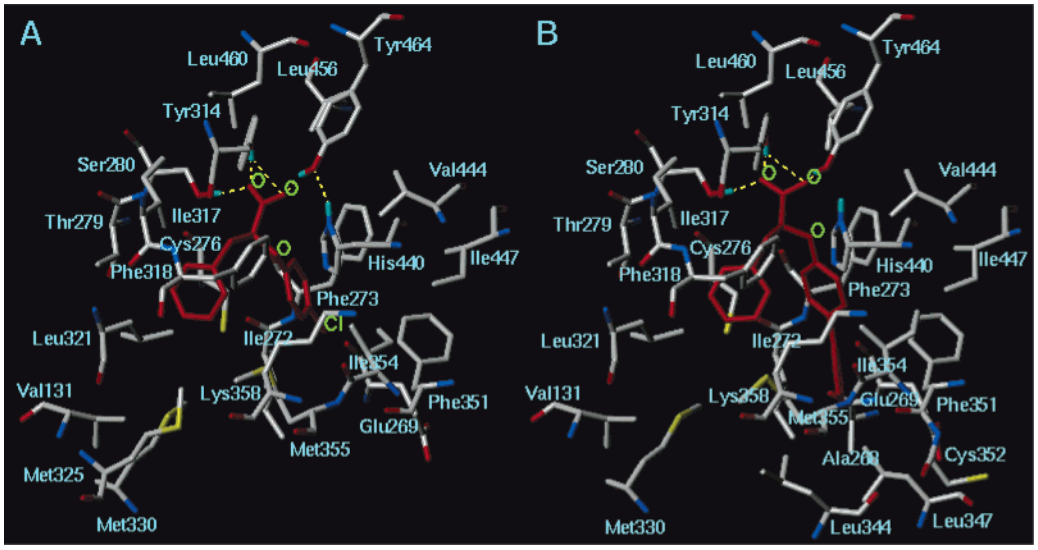

Figure 6. (*S*)-**7** (A) and **11** (B) enantiomers docked into the PPARα binding site. Only amino acids located within 5 Å distance from the bound ligand are displayed and labeled. The ligand atoms are shown in red. The hydrogen bonds discussed in the text are depicted as yellow dashed lines.

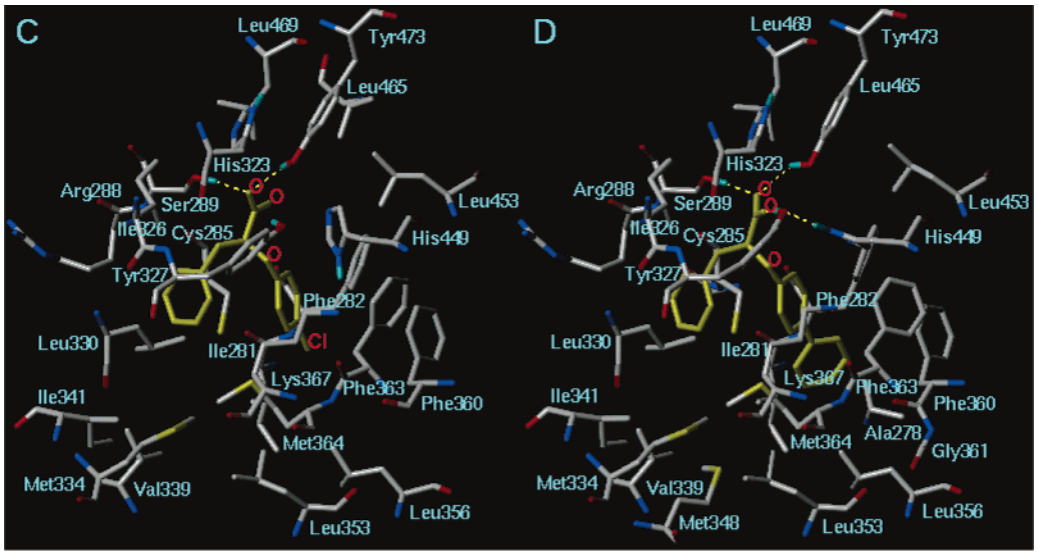

Figure 7. (*S*)-**7** (C) and **11** (D) enantiomers docked into the PPARγ binding site. Only amino acids located within 5 Å distance from the bound ligand are displayed and labeled. The ligand atoms are shown in yellow. The hydrogen bonds discussed in the text are depicted as yellow dashed lines.

To understand the hPPARγ activity and investigate possible binding modes, compounds (*S*)-**7** and **11** were also docked into the hPPARγ. AutoDock showed that a very clear preference for a single position in the active site could be obtained for (*S*)-**7**: the result with top binding energy (−8.5 kcal/mol) was found 36 times out of 50 (Table 2). The structure of the ligand revealed a binding mode very similar to that previously described for (*S*)-**7** into PPARα (Figure 7C). The carboxylic group of (*S*)-**7** is involved in hydrogen bonds with Tyr473 and Ser289. The side chains of His323 (Tyr314 in PPARα) and His449 (His440 in PPARα), which are involved in hydrogen bond formation in other PPARγ receptor/ligand complexes,[48−50] appear somewhat too far away for significant hydrogen-bonding contributions so that the activation of the receptor by the ligand could be only partial, explaining thus the partial agonist properties of (*S*)-**7** at PPARγ.

This different binding mode of the ligand within the PPARγ receptor seems, therefore, to exclude the hypothesis of a covalent interaction with the receptor at the level of the chlorine atom as previously described for an irreversible PPARγ ligand,[51] for which a specific cysteine residue was identified as the attachment site. On the other hand, differently from that compound, in our series the replacement of the chlorine in (*S*)-**7** with other substituents still retains the PPARγ activity. Figure 8 shows a superimposition of (*S*)-**7** on rosiglitazone bound to the PPARγ with only the residues involved in hydrogen bonding. The benzyl and 4-chlorophenoxy rings of (*S*)-**7** occupy the two previously described hydrophobic pockets.

Phe363 and Phe282 are involved in hydrophobic contacts with the 4-chlorophenoxy ring of the ligand. Particularly, the benzene ring of Phe363 makes a favorable π-stacking interaction with the aromatic ring of (*S*)-**7**. The Phe282 side chain also interacts with the aromatic ring of the ligand via a T-shaped interaction. Such interactions would be consistent with the activity trend of these compounds showing that lipophilic and

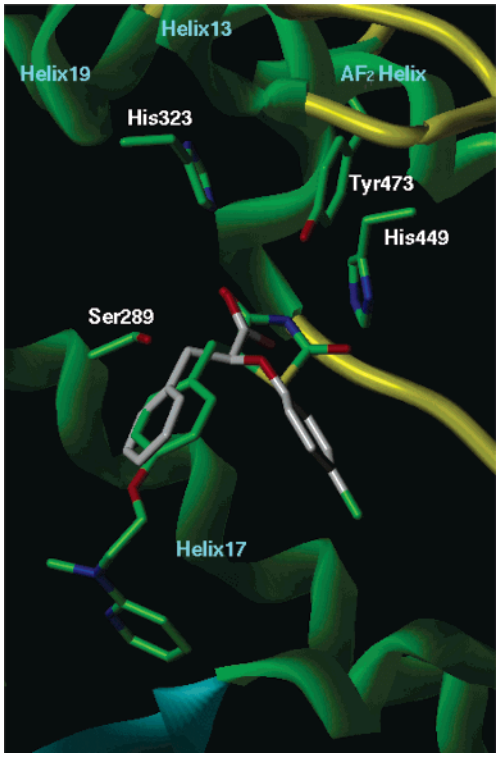

Figure 8. Superimposition of (*S*)-enantiomer of **7** (by-atom) on the PPARγ-bound conformation of rosiglitazone[48] (green). Indicated are also the residues involved in hydrogen bonding to (*S*)-**7**, with their residue types and sequence numbers written in white, and the numbers of the helices in the active site region written in cyan.

electron-withdrawing substituents in the para position of the phenoxy ring increase the potency. In fact, the electron-withdrawing trifluoromethyl group of compound **8** allows to favorably realize a π-stacking charge-transfer interaction with the electron-rich ring of Phe363.

In case of **11**, AutoDock furnished two top-ranked clusters. Besides the top result with a Δ*G* of −10.3 kcal/mol (found 10 times out of 50), a second result is obtained with a Δ*G* of −10.7 kcal/mol (found 7 times). Interestingly, both results are located in the active site and share the binding mode of (*S*)-**7**, respectively. In contrast to the results observed for (*S*)-**7**, the carboxylic group of **11** forms hydrogen bonds with Ser289, Tyr327, and Tyr473. His449 is involved in indirect recognition of the ligand, which is mediated through Tyr327. In fact, the O^{η} of this tyrosine is hydrogen bonded with the $N^{\epsilon}2$ of His449 (Figure 7D). These results support the crucial role of the hydrogen bonding pattern involving the four residues mentioned above for ligand binding and agonist activity of **11** in PPARγ.

The lower potency and efficacy of (*S*)-**7** on PPARγ compared to rosiglitazone, however, could be a favorable peculiarity of this molecule as well as its dual PPARα/PPARγ activity. Differently, in fact, from conventional PPARγ agonists or antagonists, (*S*)-**7** could behave as a PPARγ modulator, that is a ligand able to suitably act as a full agonist, partial agonist or antagonist based on the tissue involved. Compounds with this pharmacological profile have been previously described and, in some cases, were found to display a partial PPARγ agonism together with lower adipogenic effect than rosiglitazone but similar or greater insulin-sensitizing activity.[36,38,50,52−56]

In conclusion, we prepared a new series of chiral clofibric acid analogues some of which were potent PPARα agonists as well as PPARγ agonists. For the partial PPARγ agonist (*S*)-**7**, the lower potency and efficacy on PPARγ was associated with a lower adipogenic effect distinguishing it from conventional PPARγ agonists and suggesting it is a PPARγ modulator. In particular, due to the reduced efficiency in the stimulation of adipocyte differentiation and the ensuing fat accretion and weight gain, (*S*)-**7** could represent a very promising candidate as the lead for the design of new dual PPARα/PPARγ drugs to be used in the therapy of human metabolic disorders such as type 2 diabetes, atherosclerosis, and obesity in patients with high cardiovascular risk.

Experimental Section

Chemical Methods. Column chromatography was performed on ICN silica gel 60 Å (63−200 μm) as the stationary phase. Melting points were determined in open capillaries on a Gallenkamp electrothermal apparatus and are uncorrected. Mass spectra were recorded with a HP GC/MS 6890-5973 MSD spectrometer, electron impact 70 eV, equipped with HP chemstation. ^{1}H NMR spectra were recorded in $CDCl_3$ either on a Varian EM-390 (when 90 MHz is indicated), using tetramethylsilane as the internal standard, or on a Varian-Mercury 300 (300 MHz) spectrometer. Chemical shifts are expressed as parts per million (δ). Microanalyses of solid compounds were carried out with an Eurovector Euro EA 3000 model analyzer; the analytical results are within ±0.4% of theoretical values. Optical rotations were measured with a Perkin-Elmer 341 polarimeter at room temperature (20 °C): concentrations are expressed as g/100 mL. The enantiomeric excesses of acids were determined by HPLC analysis of their methyl esters, obtained by reaction with an ethereal solution of diazomethane, on Chiralcel OD, AD or OD-R columns (4.6 mm i.d. × 250 mm, Daicel Chemical Industries, Ltd., Tokio, Japan). For this purpose, small amounts of the (*R*)-enantiomers of **8**−**15** were also prepared starting from (*S*)-methyl phenyllactate. Analytical liquid chromatography was performed on a PE chromatograph equipped with a Rheodyne 7725i model injector, a 785A model UV/Vis detector, a series 200 model pump and NCI 900 model interface. Chemicals were from Aldrich and were used without any further purification. Complete ^{1}H NMR, MS, and elemental analysis data are given in the Supporting Information.

(*S*)-Methyl 2-(2-Naphthyloxy)pentanoate (16). A solution of diethylazodicarboxylate (DEAD, 8 mmol) in anhydrous THF (30 mL) was added dropwise to an ice-bath cooled mixture of equimolar amounts of (*R*)-methyl 2-hydroxypentanoate (prepared from (*R*)-2-hydroxypentanoic acid[40] with a solution of diazomethane in diethyl ether), 2-naphthol and triphenylphosphine in anhydrous THF (15 mL). The reaction mixture was stirred at room-temperature overnight, under N_2 atmosphere. THF was evaporated in vacuo and a mixture of Et_2O and hexane (30 mL, 1:1) was added to the residue. The resulting precipitate was filtered off and the filtrate was evaporated to dryness. The residue was chromatographed on silica gel column (petroleum ether/ethyl acetate 8:2 as eluent) affording the desired compound as a pale yellow oil in 82% yield.

The (*R*)-enantiomer of **16** was prepared with the same procedure starting from (*S*)-methyl 2-hydroxypentanoate; yield: 85%.

(*R*)-Methyl 2-(4-Bromobenzyloxy)pentanoate (17). A solution of (*R*)-2-hydroxypentanoic acid[40] (17 mmol) in anhydrous DMF (25 mL) was added dropwise, under N_2 atmosphere, to a stirred and ice-bath cooled suspension of NaH 95% powder (53 mmol) in anhydrous DMF (50 mL). After the gas

evolution had ceased, a solution of 4-bromobenzyl bromide (14 mmol) in anhydrous DMF (25 mL) was added dropwise to the mixture which was stirred overnight at room-temperature. Ethyl acetate (25 mL) was added to quench the reaction mixture which was evaporated to dryness; the residue was suspended in ethyl acetate and poured into cooled 6 N HCl. The organic layer was separated, and the aqueous phase was extracted with ethyl acetate. The collected organic phases were washed with a saturated solution of NH_4Cl and extracted with a saturated solution of $NaHCO_3$. The aqueous layer was acidified with 6 N HCl and extracted with ethyl acetate. The organic layer was dried over Na_2SO_4 and evaporated to dryness affording the crude acid as a yellow oil. After dissolving in Et_2O (10 mL), a freshly prepared diazomethane ethereal solution was added up to persistent yellow coloring. The solvent was removed under vacuum and the desired ester was obtained, as a yellow oil, after purification by column chromatography on silica gel (petroleum ether/$CHCl_3$ 7:3 and then 4:6 as eluents). Yield: 32%.

The (*S*)-enantiomer of **17** was prepared with the same procedure starting from (*S*)-2-hydroxypentanoic acid;[40] yield: 44%.

(*R*)-Methyl 2-[4-(4-Chlorophenyl)benzyloxy]pentanoate (18). A solution of **17** (2 mmol) in anhydrous toluene (3 mL) was added dropwise, in N_2 atmosphere, to a warm (80 °C) and stirred suspension of 4-chlorophenylboronic acid (4 mmol), anhydrous K_2CO_3 (3 mmol), and tetrakis(triphenylphosphine)-palladium (0.07 mmol) in anhydrous toluene (3 mL). The resulting mixture was stirred at 80 °C for 7 h and filtered on Celite which was washed with ethyl acetate. The organic solution was washed with 0.5 N NaOH, 15% citric acid, and brine, dried over Na_2SO_4, and evaporated to dryness affording a dark solid. The desired product was obtained as a yellow oil after purification by column chromatography on silica gel (petroleum ether/ethyl acetate 9.5:0.5 and then 8:2 as eluents) in 55% yield.

The (*S*)-enantiomer of **18** was prepared with the same procedure starting from the (*S*)-enantiomer of **17**; yield: 70%.

General Procedure for the Preparation of Methyl or Ethyl 2-(4-Substituted-aryloxy)-3-phenyl-propanoates (19a−i). A solution of diisopropylazodicarboxylate (DIAD, 10 mmol) in anhydrous toluene (20 mL) was added dropwise to an ice-bath cooled mixture of (*R*)-methyl or ethyl phenyllactate (10 mmol), the appropriate phenol (5 mmol), and triphenylphosphine (10 mmol) in anhydrous toluene (55 mL). The reaction mixture was stirred at room-temperature overnight, under N_2 atmosphere. Toluene was evaporated in vacuo, and a mixture of Et_2O and hexane (40 mL, 1:1) was added to the residue. The resulting precipitate was filtered off, and the filtrate was evaporated to dryness. The residue was chromatographed on silica gel column (petroleum ether/ethyl acetate 9:1 as eluent) affording the desired compounds as oils or white solids in 40−92% yields.

(*S*)-Methyl 2-(4-bromophenoxy)-3-phenyl-propanoate (19a): white solid; 76% yield.

(*S*)-Methyl 2-(4-chlorophenoxy)-3-phenyl-propanoate (19b): pale yellow oil; 72% yield.

The (*R*)-enantiomer of **19b** was prepared with the same procedure starting from (*S*)-methyl phenyllactate; yield: 68%.

(*S*)-Methyl 2-(4-trifluoromethylphenoxy)-3-phenyl-propanoate (19c): pale yellow oil; 92% yield.

(*S*)-Methyl 2-(4-Methoxyphenoxy)-3-phenyl-propanoate (19d). After column chromatography, a GC analysis of the oil obtained showed the presence of an impurity in the ratio of about 1:1. However, **19d** (45% yield, approximately, on the base of GC analysis) was used for the next step without any further purification.

(*S*)-Methyl 2-(4-acetylphenoxy)-3-phenyl-propanoate (19e): pale yellow oil; 73% yield.

(*S*)-Methyl 2-(4-phenylphenoxy)-3-phenyl-propanoate (19f): white solid; 52% yield.

(*S*)-Methyl 2-(4-ethylphenoxy)-3-phenyl-propanoate (19g): colorless oil; 40% yield.

(*S*)-Methyl 2-(2-naphthyloxy)-3-phenyl-propanoate (19h): pale yellow oil; 72% yield.

(*S*)-Ethyl 2-(4-formylphenoxy)-3-phenyl-propanoate (19i): pale yellow oil; 71% yield.

(*S*)-Methyl 2-[4-(2-Thienyl)phenoxy]-3-phenyl-propanoate. This compound was prepared by the same procedure reported for **18** starting from **19a** and 2-thiopheneboronic acid. White solid; 52% yield.

(*S*)-Ethyl 2-[4-(Hydroxymethyl)phenoxy]-3-phenyl-propanoate. To an ice-bath cooled solution of **19i** (0.76 g, 2.55 mmol) in (1:1) THF/H_2O (20 mL), $NaBH_4$ (0.096 g, 2.55 mmol) was added. The reaction mixture was stirred at 0 °C for 15 min and then was poured into brine and extracted with Et_2O. The organic layer was dried over Na_2SO_4 and evaporated in vacuo to give a yellow pale oil (0.88 g) which was chromatographed on silica gel column (petroleum ether/ethyl acetate 8:2 as eluent) affording the desired compound as a colorless oil in 72% yield.

General Procedure for the Preparation of the Final Acids. A solution of the corresponding methyl or ethyl esters (5 mmol) in THF (30 mL) and 1 N NaOH (30 mL) was stirred at room temperature for 1−6 h. The organic layer was removed under reduced pressure, and the residue was acidified with 6 N HCl and extracted with Et_2O. The organic layer was dried over Na_2SO_4 and evaporated to dryness affording the final acids as white solids which were recrystallized from hexane or $CHCl_3$/hexane (34−95% yields).

(+)-(*R*)-2-(2-Naphthyloxy)pentanoic acid [(*R*)-5]: 34% yield; mp: 139−40 °C (hexane); $[\alpha]_D = +59$ (*c* 1.0, MeOH); e.e. = 99% (methyl ester on Chiralcel OD-R column, CH_3CN/H_2O 60:40 as the mobile phase, flow rate: 0.4 mL/min, detection: 254 nm).

(−)-(*S*)-2-(2-Naphthyloxy)pentanoic acid [(*S*)-5]: 43% yield; mp: 140−2 °C (hexane); $[\alpha]_D = -59$ (*c* 1.0, MeOH); e.e. = 99% (for experimental conditions, see (*R*)-**5**).

(+)-(*R*)-2-[4-(4-Chlorophenyl)benzyloxy]pentanoic acid [(*R*)-6]: 47% yield; mp: 97−8 °C (hexane); $[\alpha]_D = +56$ (*c* 1.0, MeOH); e.e. = 98% (methyl ester on Chiralcel AD column, hexane/*i*-PrOH 98:2 as the mobile phase, flow rate: 0.5 mL/min, detection: 254 nm).

(−)-(*S*)-2-[4-(4-Chlorophenyl)benzyloxy]pentanoic acid [(*S*)-6]: 50% yield; mp: 99−100 °C (hexane); $[\alpha]_D = -58$ (*c* 1.0, MeOH); e.e. = 99% (for experimental conditions, see (*R*)-**6**).

(+)-(*R*)-2-(4-Chlorophenoxy)-3-phenyl-propanoic acid [(*R*)-7]: 42% yield; mp: 117−8 °C ($CHCl_3$/hexane); $[\alpha]_D = +12$ (*c* 1.0, MeOH); e.e. = 98% (methyl ester on Chiralcel OD column, hexane/*i*-PrOH 98:2 as the mobile phase, flow rate: 0.5 mL/min, detection: 230 nm).

(−)-(*S*)-2-(4-Chlorophenoxy)-3-phenyl-propanoic acid [(*S*)-7]: 60% yield; mp: 116−7 °C ($CHCl_3$/hexane); $[\alpha]_D = -13$ (*c* 1.0, MeOH); e.e. = 99% (for experimental conditions, see (*R*)-**7**).

(−)-(*S*)-2-(4-Trifluoromethylphenoxy)-3-phenyl-propanoic acid (8): 95% yield; mp: 117−8 °C ($CHCl_3$/hexane); $[\alpha]_D = -17$ (*c* 1.0, MeOH); e.e. = 99% (methyl ester on Chiralcel OD column, hexane/*i*-PrOH 98:2 as the mobile phase, flow rate: 0.5 mL/min, detection: 230 nm).

(−)-(*S*)-2-(4-Methoxyphenoxy)-3-phenyl-propanoic acid (9): 34% yield; mp: 94−5 °C ($CHCl_3$/hexane); $[\alpha]_D = -11$ (*c* 1.0, MeOH); e.e. = 98% (methyl ester on Chiralcel OD column, hexane/*i*-PrOH 98:2 as the mobile phase, flow rate: 0.5 mL/min, detection: 230 nm).

(−)-(*S*)-2-(4-Acetylphenoxy)-3-phenyl-propanoic acid (10): 74% yield; mp: 90−1 °C ($CHCl_3$/hexane); $[\alpha]_D = -15$ (*c* 1.0, MeOH); e.e. = 98% (methyl ester on Chiralcel AD column, hexane/*i*-PrOH 90:10 as the mobile phase, flow rate: 0.5 mL/min, detection: 280 nm).

(−)-(*S*)-2-(4-Phenylphenoxy)-3-phenyl-propanoic acid (11): 76% yield; mp: 149−50 °C ($CHCl_3$/hexane); $[\alpha]_D = -1$ (*c* 1.0, MeOH); e.e. = 99% (methyl ester on Chiralcel OD column, hexane/*i*-PrOH 98:2 as the mobile phase, flow rate: 0.5 mL/min, detection: 230 nm).

(−)-(*S*)-2-(4-Ethylphenoxy)-3-phenyl-propanoic acid (12): 72% yield; mp: 84−5 °C (hexane); $[\alpha]_D = -10$ (*c* 1.0, MeOH); e.e. = 97% (methyl ester on Chiralcel AD column, hexane/*i*-PrOH 98:2 as the mobile phase, flow rate: 1 mL/min, detection: 225 nm).

(−)-(*S*)-2-[4-(Hydroxymethyl)phenoxy]-3-phenyl-propanoic acid (13): 80% yield; mp: 128−9 °C ($CHCl_3$/hexane); $[\alpha]_D = -12$ (*c* 1.0, MeOH); e.e. = 99% (methyl ester on Chiralcel AD column, hexane/*i*-PrOH 95:5 as the mobile phase, flow rate: 1 mL/min, detection: 280 nm).

(+)-(*S*)-2-[4-(2-Thienyl)phenoxy]-3-phenyl-propanoic acid (14): 44% yield; mp: 154−5 °C ($CHCl_3$/hexane); $[\alpha]_D = +8$ (*c* 1.0, MeOH); e.e. = 99% (methyl ester on Chiralcel OD column, hexane/*i*-PrOH 90:10 as the mobile phase, flow rate: 0.5 mL/min, detection: 230 nm).

(+)-(*S*)-2-(2-Naphthyloxy)-3-phenyl-propanoic acid (15): 76% yield; mp: 133−4 °C ($CHCl_3$/hexane); $[\alpha]_D = +19$ (*c* 1.0, MeOH); e.e. = 99% (methyl ester on Chiralcel OD column, hexane/*i*-PrOH 98:2 as the mobile phase, flow rate: 0.5 mL/min, detection: 230 nm).

Biological Methods. Medium and other cell culture reagents, Wy-14,643, clofibric acid, insulin, dexamethasone and isobutylmethylxanthin (IBMX) were purchased from Sigma (St. Louis, MO). BRL 49653 (rosiglitazone) was obtained by Hefei Scenery Chemical Co. (Hefei, Anhui, Popular Republic of China).

Plasmids. The expression vectors expressing the chimeric receptors containing the yeast GAL4-DNA binding domain fused to either the human PPARα/PPARγ ligand binding domain (LBD) and the reporter plasmid for these GAL4 chimeric receptors (pGAL5TKpGL3) containing five repeats of the GAL4 response elements upstream of a minimal thymidine kinase promoter that is adjacent to the luciferase gene were described previously.[57] The murine PPARα LBD and the human PPARδ LBD expression plasmids in the pSG5 vector were kind gifts from Dr. Krister Bamberg (AstraZeneca, Mölndal, Sweden).

Cell Culture and Transfections. Human hepatoblastoma cell line HepG2 (American Type Culture Collection, Manassas, VA) was cultured in Dulbecco's Modified Eagle Media/F-12 Nutrient (1:1) Mixture (D-MEM/F-12) containing 10% of heat inactivated Foetal Calf Serum, 100 U penicillin G/mL and 100 μg streptomycin sulfate/mL at 37 °C in a humidified atmosphere of 10% CO_2. For transactivation assay 10^5 cells/well were seeded in a 24 well plate in triplicate and transfections were performed with a modification of the calcium-phosphate method.[58] Cells were transfected with expression plasmids encoding the fusion protein GAL4-PPARα LBD or GAL4-PPARγ LBD (30 ng), pGAL5TKpGL3 (100 ng), pCMVβgal (300 ng). After transfection, cells were treated for 20 h with the indicated ligands. Luciferase activity in cell extracts was then determined by a luminometer (LUMAT LB 9501 Berthold). β-Galactosidase activity was determined using β-D-galactopyranoside (Calbiochem) as described previously.[59] All transfection experiments were repeated at least twice.

3T3-L1 Differentiation. Murine fibroblast 3T3-L1 cells from American Type Culture Collection were cultured in D-MEM with 10% heat inactivated bovine calf serum, 100 U penicillin G/mL, and 100 μg streptomycin sulfate/mL at 37 °C in a humidified atmosphere of 10% CO_2. For differentiation experiments, 6×10^4 cells/well were seeded in six-well plates in duplicate. After reaching confluence, usually after 5−6 days, cells were stimulated to differentiate as described.[60] Briefly, 2 days postconfluent preadipocytes were treated with complete medium containing 1 μM dexamethasone, 1 μM IBMX, and 2 μM insulin (DEX/MIX medium). After 2 days, the DEX/MIX medium was removed, cells were washed three times with medium and then treated with ligands for 10 days. Medium was replenished with appropriate ligands every 2 days.

Limited Proteolysis Digestion Analysis. Protease digestion was carried out as described previously[44] with minor modifications. The plasmid pGAL4-hPPARγ LBD was used to synthesize ^{35}S-radiolabeled PPARγ in a coupled transcription/translation system according to the protocol of the manufacturer (Promega). The transcription/translation reaction was subsequently aliquoted and ethanol or rosiglitazone or compound (*S*)-**7** was added. These mixtures were incubated for 20 min at 25 °C. The protease was added and digestions were allowed to proceed for 10 min at 25 °C. The reactions were terminated by the addition of gel loading buffer and boiling for 5 min. The products of the digestion were separated by electrophoresis through a 12% polyacrylamide-SDS gel. After electrophoresis, the gel was dried and the radiolabeled digestion products were visualized by autoradiography.

Computational Chemistry. Molecular modeling and graphics manipulations were performed using the SYBYL software package (Sybyl Molecular Modeling System, version 6.9, Tripos Inc., St. Louis, MO), running it on a Silicon Graphics R12000 workstation. Model building of (*S*)-**7** and **11** was accomplished with the TRIPOS force field[61] available within SYBYL. Point charges were calculated as Kollman-all-atom[62] for proteins and Gasteiger-Marsili[63] for ligands. Energy minimizations were realized by employing the Insight II/Discover program (Insight II Molecular Modeling Package and Discover 2.2000 Simulation Package, MSI Inc., San Diego, CA), selecting the CVFF force field.[64]

Docking Simulations. Docking was performed with version 3.05 of the program AutoDock.[47] It combines a rapid energy evaluation through precalculated grids of affinity potentials with a variety of search algorithms to find suitable binding positions for a ligand on a given protein. While the protein is required to be rigid, the program allows torsional flexibility in the ligand.

Docking to PPARα and PPARγ was carried out using the empirical free energy function and the Lamarckian genetic algorithm, applying a standard protocol, with an initial population of 50 randomly placed individuals, a maximum number of 1.5×10^6 energy evaluations, a mutation rate of 0.02, a crossover rate of 0.80, and an elitism value of 1. Proportional selection was used, where the average of the worst energy was calculated over a window of the previous 10 generations. For the local search, the so-called pseudo-Solis and Wets algorithm was applied using a maximum of 300 iterations per local search. The probability of performing local search on an individual in the population was 0.06, and the maximum number of consecutive successes or failures before doubling or halving the local search step size was 4. Fifty independent docking runs were carried out for each ligand. Results differing by less than 1.5 Å in positional root mean-square deviation (rmsd) were clustered together and represented by the result with the most favorable free energy of binding.

(1) Ligand Setup. Molecular models of compounds (*S*)-**7** and **11** were constructed using standard bond lengths and bond angles of the SYBYL fragment library. The carboxylate group was taken as dissociated. Geometry optimizations were realized with the SYBYL/MAXIMIN2 minimizer by applying the BFGS (Broyden, Fletcher, Goldfarb, and Shannon) algorithm and setting an rms gradient of the forces acting on each atom of 0.05 kcal/mol Å as the convergence criterion. Atomic charges were assigned using the Gasteiger-Marsili formalism,[63] which is the type of atomic charges used in calibrating the AutoDock empirical free energy function. Finally, the compounds were setup for docking with the help of AutoTors, the main purpose of which is to define the torsional degrees of freedom to be considered during the docking process. The number of flexible torsions defined for each ligand is as follow: five in (*S*)-**7** and six in **11**.

(2) Protein Setup. Crystal structures of PPARα in complex with GW409544 (entry code: 1K7L)[46] and PPARγ in complex with rosiglitazone (entry code: 1KNU),[21] recovered from Brookhaven Protein Database, were used. The structures were setup for docking as follows: polar hydrogens were added using the PROTONATE utility.[47] To optimize the hydrogen positions, the structures were subjected to a short energy minimization using the Discover module of InsightII, in accordance with the type of force field and protein charges of the AutoDock empirical free energy function. Solvation parameters were

added to the final protein file using the ADDSOL utility of AutoDock 3.05. The grid maps representing the proteins in the actual docking process were calculated with AutoGrid. The grids (one for each atom type in the ligand, plus one for electrostatic interactions) were chosen to be sufficiently large to include not only the active site but also significant portions of the surrounding surface. The dimensions of the grids were thus 30 Å × 30 Å × 30 Å, with a spacing of 0.375 Å between the grid points. Refinement of the receptor/ligand complexes was achieved by energy minimization using the steepest descent and conjugate gradient methods, permitting only the ligand and the side chain atoms of the protein to relax.

Acknowledgment. This work was accomplished thanks to the financial support of the Ministero dell'Istruzione, dell'Università e della Ricerca (MIUR 2003033405), and of the University of Milano (FIRST2003/2004 to M.C.).

Supporting Information Available: Spectroscopic data for intermediates and final compounds and microanalysis data for acids **5**−**15**. This material is available free of charge via the Internet at http:// pubs.acs.org.

References

(1) De Franzo, R. A.; Bonadonna, R. C.; Ferrannini, E. Pathogenesis of NIDDM. *Diabetes Care* **1992**, *15*, 318−368.
(2) Eriksson, J.; Franssila-Kallunki, A.; Ekstrand, A.; Saloranta, C.; Widen, E.; Schalin, C.; Groop, L. Early metabolic defects in persons at increased risk for non-insulin-dependent diabetes mellitus. *N. Engl. J.* Med. **1989**, *321*, 337−343.
(3) Lillioja, S.; Mott, D. M.; Spraul, M.; Ferraro, R.; Foley, J. E.; Ravussin, E.; Knowler, W. C.; Bennett, P. H.; Bogardus, C. Insulin resistance and insulin secretory dysfunction as precursors of non-insulin-dependent diabetes mellitus. Prospective studies of Pima Indians. *N. Engl. J. Med.* **1993**, *329*, 1988−1992.
(4) Pimenta, W.; Korytkowski, M.; Mitrakou, A.; Jenssen, T.; Yki-Jarvinen, H.; Evron, W.; Dailey, G.; Gerich, J. Pancreatic beta-cell dysfunction as the primary genetic lesion in NIDDM. Evidence from studies in normal glucose-tolerant individuals with a first-degree NIDDM relative. *JAMA* **1995**, *273*, 1855−1861.
(5) Fernandez-Castaner, M.; Biarnes, J.; Camps, I.; Ripolles, J.; Gomez, N.; Soler, J. Beta-cell dysfunction in first-degree relatives of patients with non-insulin-dependent diabetes mellitus. *Diabet. Med.* **1996**, *13*, 953−959.
(6) Volk, A.; Renn, W.; Overkamp, D.; Mehnert, B.; Maerker, E.; Jacob, S.; Balletshofer, B.; Haring, H. U.; Rett, K. Insulin action and secretion in healthy, glucose tolerant first degree relatives of patients with type 2 diabetes mellitus. Influence of body weight. *Exp. Clin. Endocrinol. Diabetes* **1999**, *107*, 140−147.
(7) Weyer, C.; Bogardus, C.; Mott, D. M.; Pratley, R. E. The natural history of insulin secretory dysfunction and insulin resistance in the pathogenesis of type 2 diabetes mellitus. *J. Clin. Invest.* **1999**, *104*, 787−794.
(8) Weyer, C.; Tataranni, P. A.; Bogardus, C.; Pratley, R. E. Insulin resistance and insulin secretory dysfunction are independent predictors of worsening of glucose tolerance during each stage of type 2 diabetes development. *Diabetes Care* **2001**, *24*, 89−94.
(9) Reaven, G. M. Role of insulin resistance in human desease. *Diabetes* **1988**, *37*, 1597−1607.
(10) Moneva, M. H.; Dagogo-Jack, S. Multiple drug targets in the management of type 2 diabetes. *Curr. Drug Targets* **2002**, *3*, 203−221.
(11) Hulin, B. New hypoglycaemic agents. *Prog. Med. Chem.* **1994**, *31*, 1−58.
(12) Issemann, I.; Green, S. Activation of a member of the steroid hormone receptor superfamily by peroxisome proliferators. *Nature* **1990**, *347*, 645−650.
(13) Kliewer, S. A.; Umesono, K.; Noonan, D. J.; Heyman, R. A.; Evans, R. M. Convergence of 9-*cis*-retinoic acid and peroxisome proliferator signaling pathways through heterodimer formation of their receptors. *Nature* **1992**, *358*, 771−774.
(14) Mangelsdorf, D. J.; Evans, R. M. The RXR heterodimers and orphan receptors. *Cell* **1995**, *83*, 841−850.
(15) Staels, B.; Dallongeville, J.; Auwerx, J.; Schoonjans, K.; Leitersdorf, E.; Fruchart, J.-C. Mechanism of action of fibrates on lipid and lipoprotein metabolism. *Circulation* **1998**, *98*, 2088−2093.
(16) Fruchart, J.-C.; Duriez, P.; Staels, B. Peroxisome proliferator-activated receptor-alpha activators regulate genes governing lipoprotein metabolism, vascular inflammation and atherosclerosis. *Curr. Opin. Lipidol.* **1999**, *10*, 245−257.
(17) Willson, T. M.; Cobb, J. E.; Cowan, D. J.; Wiethe, R. W.; Correa, I. D.; Prakash, S. R.; Beck, K. D.; Moore, L. B.; Kliewer, S. A.; Lehmann, J. M. The Structure−Activity Relationship between Peroxisome Proliferator-Activated Receptor γ Agonism and the Antihyperglycemic Activity of Thiazolidinediones. *J. Med. Chem.* **1996**, *39*, 665−668.
(18) Cronet, P.; Petersen, J. F. W.; Folmer, R.; Blomberg, N.; Sjöblom, K.; Karlsson, U.; Lindstedt, E.-L.; Bamberg, K. Structure of the PPARα and -γ ligand binding domain in complex with AZ 242: Ligand selectivity and Agonist Activation in the PPAR family. *Structure* **2001**, *9*, 699−706.
(19) Brooks, D. A.; Etgen, G. J.; Rito, C. J.; Shuker, A.; Dominianni, S. J.; Warshawsky, A. M.; Ardecky, R.; Paterniti, J. R.; Tyhonas, J.; Karanewsky, D. S.; Kauffman, R. F.; Broderick, C. L.; Oldham, B. A.; Montrose-Rafizadeh, C.; Winneroski, L. L.; Faul, M. M.; McCarthy, J. R. Design and Synthesis of 2-Methyl-2-{4-[2-(5-methyl-2-aryloxazol-4-yl)ethoxy]phenoxy}propionic Acids: A New Class of Dual PPARα/γ Agonists. *J. Med. Chem.* **2001**, *44*, 2061−2064.
(20) Lohray, B. B.; Lohray, V. B.; Bajji, A. C.; Kalchar, S.; Poondra, R. R.; Padakanti, S.; Chakrabarti, R.; Vikramadithyan, R. K.; Misra, P.; Juluri, S.; Mamidi, N. V. S. R.; Rajagopalan, R. (−)3-[4-[2-(Phenoxazin-10-yl)ethoxy]phenyl]-2-ethoxypropanoic Acid [(−)DRF2725]: A Dual PPAR Agonist with Potent Antihyperglycemic and Lipid Modulating Activity. *J. Med. Chem.* **2001**, *44*, 2675−2678.
(21) Sauerberg, P.; Pettersson, I.; Jeppesen, L.; Bury, P. S.; Mogensen, J. P.; Wassermann, K.; Brand, C. L.; Sturis, J.; Wöldike, H. F.; Fleckner, J.; Andersen, A.-S. T.; Mortensen, S. B.; Svensson, L. A.; Rasmussen, H. B.; Lehmann, S. V.; Polivka, Z.; Sindelar, K.; Panajotova, V.; Ynddal, L.; Wulff, E. M. Novel Tricyclic-α-alkyloxyphenylpropionic Acids: Dual PPAR α/γ Agonists with Hypolipidemic and Antidiabetic Activity. *J. Med. Chem.* **2002**, *45*, 789−804.
(22) Etgen, G. J.; Oldham, B. A.; Johnson, W. T.; Broderick, C. L.; Montrose, C. R.; Brozinick, J. T.; Misener, E. A.; Bean, J. S.; Bensch, W. R.; Brooks, D. A.; Shuker, A. J.; Rito, C. A.; McCarthy, J. R.; Ardecky, R. A.; Tyhonas, J. S.; Dana, S. L.; Bilakovics, J. M.; Paterniti, J. R., Jr.; Ogilvie, K. M.; Liu, S.; Kauffman, R. F. A Tailored Therapy for the Metabolic Syndrome, The Dual Peroxisome Proliferator-Activated Receptor-α/γ Agonist LY465608 Ameliorates Insulin Resistance and Diabetes Hyperglycemia While Improving Cardiovascular Risk Factors in Preclinical Models. *Diabetes* **2002**, *51*, 1083−1087.
(23) Ebdrup, S.; Pettersson, I.; Rasmussen, H. B.; Deussen, H.-J.; Jensen, A. F.; Mortensen, S. B.; Fleckner, J.; Pridal, L.; Nygaard, L.; Sauerberg, P. Synthesis and Biological and Structural Characterization of the Dual-Acting Peroxisome Proliferator-Activated Receptor α/γ Agonist Ragaglitazar. *J. Med. Chem.* **2003**, *46*, 1306−1317.
(24) Xu, Y.; Rito, C. J.; Etgen G. J.; Ardecky, R. J.; Bean, J. S.; Bensch, W. R.; Bosley, J. R.; Broderick, C. L.; Brooks, D. A.; Dominianni, S. J.; Hahn, P. J.; Liu, S.; Mais, D. E.; Montrose-Rafizadeh, C.; Ogilvie, K. M.; Oldham, B. A.; Peters, M.; Rungta, D. K.; Shuker, A. J.; Stephenson, G. A.; Tripp, A. E.; Wilson, S. B.; Winneroski, L. L.; Zink, R.; Kauffman, R. F.; McCarthy, J. R. Design and Synthesis of α-Aryloxy-α-methylhydrocinnamic Acids: A Novel Class of Dual Peroxisome Proliferator-Activated Receptor α/γ Agonists. *J. Med. Chem*. **2004**, *47*, 2422−2425.
(25) Koyama, H.; Miller, D. J.; Boueres, J. K.; Desai, R. C.; Jones, B.; Berger, J. P.; MacNaul, K. L.; Kelly, L. J.; Doebber, T. W.; Wu, M. S.; Zhou, G.; Wang, P.; Ippolito, M. C.; Chao, Y.-S.; Agrawal, A. K.; Franklin, R.; Heck, J. V.; Wright, S. D.; Moller, D. E.; Sahoo, S. P. (2*R*)-2-Ethylchromane-2-carboxylic acids: Discovery of Novel PPARα/γ Dual Agonists as Antihyperglycemic and Hypolipidemic Agents. *J. Med. Chem*. **2004**, *47*, 3255−3263.
(26) Takamura, M.; Sakurai, M.; Yamada, E.; Fujita, S.; Yachi, M.; Takagi, T.; Isobe, A.; Hagisawa, Y.; Fujiwara, T.; Yanagisawa, H. Synthesis and biological activity of novel α-substituted β-phenylpropionic acids having pyridin-2-ylphenyl moiety as antihyperglycemic agents. *Bioorg. Med. Chem.* **2004**, *12*, 2419−2439.
(27) Murakami, K.; Tobe, K.; Ide, T.; Mochizuki, T.; Ohashi, M.; Akanuma, Y.; Yazaki, Y.; Kadowaki, T. A novel insulin sensitizer acts as a coligand for peroxisome proliferator-activated receptor-α (PPAR-α) and PPAR-γ: effect of PPAR-α activation on abnormal lipid metabolism in liver of Zucker fatty rats. *Diabetes* **1998**, *47*, 1841−1847.
(28) Liu, K. G.; Smith, J. S.; Ayscue, A. H.; Henke, B. R.; Lambert, M. H.; Leesnitzer, L. M.; Plunket, K. D.; Willson, T. M.; Sternbach, D. D. Identification of a Series of Oxadiazole-Substituted α-Isopropoxy Phenylpropanoic Acids with Activity on PPARα, PPARγ, and PPARδ. *Bioorg. Med. Chem. Lett.* **2001**, *11*, 2385−2388.
(29) Willson, T. M.; Brown, P. J.; Sternbach, D. D.; Henke, B. R. The PPARs: From Orphan Receptors to Drug Discovery. *J. Med. Chem.* **2000**, *43*, 527−550.

(30) Rangwala, S. M.; O′Brien, M. L.; Tortorella, V.; Loiodice, F.; Longo, A.; Noonan, D. J.; Feller, D. R. Stereoselective effects of chiral clofibric acid analogues on rat peroxisome proliferator-activated receptor α (rPPARα) activation and peroxisomal fatty acid β-oxidation. *Chirality* **1997**, *9*, 37−47.
(31) Liu, K.; Xu, L.; Jones, A. B. Preparation of 1,2-benzoxazolyloxy-acetic acids and analogues as PPAR agonists for treatment of diabetes and lipid disorders. Merck & Co. Inc., USA, PCT Int. Appl. 2001, WO 0160807; *Chem. Abstr.* **2001**, *135*, 180757.
(32) Adams, A. D.; Hu, Z.; von Langen, D.; Dadiz, A.; Elbrecht, A.; MacNaul, K. L.; Berger, J. P.; Zhou, G.; Doebber, T. W.; Meurer, R.; Forrest, M. J.; Moller, D. E.; Jones, A. B. O-arylmandelic acids as highly selective human PPAR alpha/gamma agonists. *Bioorg. Med. Chem. Lett.* **2003**, *13*, 3185−3190.
(33) Wulff, E. M.; Jeppesen, L.; Bury, P. S.; Mogensen, J. P.; Fleckner, J.; Andersen, A.-S. T.; Wassermann, K.; Sauerberg, P. Characterization of a future generation insulin sensitizers in vitro and in vivo. *Diabetes* **2001**, *50* (Suppl. 2), Abst. 2210-PO.
(34) Sorbera, L. A.; Castañer, J.; del Fresno, M.; Silvestre, J. Netoglitazone. *Drugs Future* **2002**, *27*, 132−139.
(35) Luskey, K. L.; Luo, J. Preparation and use of (−)-(3-trihalomethylphenoxy)(4-halophenyl)acetates for treatment of insulin resistance, type 2 diabetes, hyperlipidemia and hyperuricemia. Metabolex, Inc., USA.; Diatex, Inc., U.S. Pat. Appl. 20030220399, 2003; *Chem. Abstr. 140*, 4856.
(36) Karpf, D. B.; Flores-Lozano, F.; Rosenstock, J. MBX-102, a novel insulin sensitizer for type 2 diabetes that does not cause weight gain or edema. Presented at the 3rd International Symposium on PPARs: Efficacy and Safety, Monte Carlo (Monaco), March 19−23, 2005. See also http://www.metabolex.com/pipeline.html.
(37) Buckle, D. R.; Cantello, B. C. C.; Cawthorne, M. A.; Coyle, P. J.; Dean, D. K.; Faller, A.; Haigh, D.; Hindley, R. M.; Jefcott, L. J.; Lister, C. A.; Pinto, I. L.; Rami, H. K.; Smith, D. G.; Smith, S. A. Non thiazolidinedione antihyperglycemic agents. 1: α-Heteroatom substituted β-phenylpropanoic acids. *Bioorg. Med. Chem. Lett.* **1996**, *6*, 2121−2126.
(38) Rocchi, S.; Picard, F.; Vamecq, J.; Gelman, L.; Potier, N.; Zeyer, D.; Dubuquoy, L.; Bac, P.; Champy, M.-F.; Plunket, K. D.; Leesnitzer, L. M.; Blanchard, S. G.; Desreumaux, P.; Moras, D.; Renaud, J.-P.; Auwerx, J. A unique PPARγ ligand with potent insulin-sensitizing yet weak adipogenic activity. *Mol. Cell* **2001**, *8*, 737−747.
(39) Cobb, J. E.; Blanchard, S. G.; Boswell, E. G.; Brown, K. K.; Charifson, P. S.; Cooper, J. P.; Collins, J. L.; Dezube, M.; Henke, B. R.; Hull-Ryde, E. A.; Lake, D. H.; Lenhard, J. M.; Oliver, W., Jr.; Oplinger, J.; Pentti, M.; Parks, D. J.; Plunket, K. D.; Tong, W.-Q. *N*-(2-Benzoylphenyl)-L-tyrosine PPAR Agonists. 3. Structure−Activity Relationship and Optimization of the *N*-Aryl Substituent. *J. Med. Chem.* **1998**, *41*, 5055−5069.
(40) Winitz, M.; Bloch-Frankenthal, L.; Izumiya, N.; Birnbaum, S. M.; Baker, C. G.; Greenstein, J. P. Studies on diastereoisomeric α-amino acids and corresponding α-hydroxy acids. VII. Influence of β-configuration on enzymic susceptibility. *J. Am. Chem. Soc.* **1956**, *78*, 2423−2430.
(41) Lehmann, J. M.; Moore, L. B.; Smith-Oliver, T. A.; Wilkinson, W. O.; Willson, T. M.; Kliewer, S. A. An antidiabetic thiazolidinedione is a high affinity ligand for peroxisome proliferator-activated receptor γ (PPARγ). *J. Biol. Chem.* **1995**, *270*, 12953−12956.
(42) Brun, R. P.; Kim, J. B.; Hu, E.; Spiegelman, B. M. Peroxisome proliferator-activated receptor γ and the control of adipogenesis. *Curr. Opin. Lipidol.* **1997**, *8*, 212−218.
(43) Camp, H. S.; Chaudhry, A.; Leff, T. A novel potent antagonist of peroxisome proliferator-activated receptor γ blocks adipocyte differentiation but does not revert the phenotype of terminally differentiated adipocytes. *Endocrinology* **2001**, *142*, 3207−3213.
(44) Allan, G. F.; Xiaohua, L.; Tsai, S. Y.; Weigel, N. L.; Edwards, D. P.; Tsai, M.-J.; O′Malley, B. W. Hormone and antihormone induce distinct conformational changes which are central to steroid receptor activation. *J. Biol. Chem.* **1992**, *267*, 19513−19520.
(45) Berger, J.; Bailey, P.; Biswas, C.; Cullinan, C. A.; Doebber, T. W.; Hayes, N. S.; Saperstein, R.; Smith, R. G.; Leibowitz, M. D. Thiazolidinediones produce a conformational change in peroxisomal proliferator-activated receptor-γ: binding and activation correlate with antidiabetic actions in db/db mice. *Endocrinology* **1996**, *137*, 4189−4195.
(46) Xu, H. E.; Lambert, M. H.; Montana, V. G.; Plunket, K. D.; Moore, L. B.; Collins, J. L.; Oplinger, J. A.; Kliewer, S. A.; Gampe, R. T., Jr.; McKee, D. D.; Moore, J. T.; Willson, T. M. Structural determinants of ligand binding selectivity between the peroxisome proliferator-activated receptors. *Proc. Natl. Acad.* Sci. *U.S.A.* **2001**, *98*, 13919−13924.
(47) Morris, G. M.; Goodsell, D. S.; Halliday, R. S.; Huey, R.; Hart, W. E.; Belew, R. K.; Olson, A. J. Automated docking using a Lamarckian genetic algorithm and an empirical binding free energy function. *J. Comput. Chem.* **1998**, *19*, 1639−1662.
(48) Nolte, R. T.; Wisely, G. B.; Westin, S.; Cobb, J. E.; Lambert, M. H.; Kurokawa, R.; Rosenfeld, M. G.; Willson, T. M.; Glass, C. K.; Milburn, M. V. Ligand binding and co-activator assembly of the peroxisome proliferator-activated receptor-gamma. *Nature* **1998**, *395*, 137−143.
(49) Xu, H. E.; Lambert, M. H.; Montana, V. G.; Parks, D. J.; Blanchard, S. G.; Brown, P. J.; Sternbach, D. D.; Lehmann, J. M.; Wisely, G. B.; Willson, T. M.; Kliewer, S. A.; Milburn, M. V. Molecular recognition of fatty acids by peroxisome proliferator-activated receptors. *Mol. Cell* **1999**, *3*, 397−403.
(50) Oberfield, J. L.; Collins, J. L.; Holmes, C. P.; Goreham, D. M.; Cooper, J. P.; Cobb, J. E.; Lenhard, J. M.; Hull-Ryde, E. A.; Mohr, C. P.; Blanchard, S. G.; Parks, D. J.; Moore, L. B.; Lehmann, J. M.; Plunket, K.; Miller, A. B.; Milburn, M. V.; Kliewer, S. A.; Willson, T. M. A peroxisome proliferator-activated receptor γ ligand inhibits adipocyte differentiation. *Proc. Natl. Acad. Sci. U.S.A.* **1999**, *96*, 6102−6106.
(51) Elbrecht, A.; Chen, Y.; Adams, A.; Berger, J.; Griffin, P.; Klatt, T.; Zhang, B.; Menke, J.; Zhou, G.; Smith, R. G.; Moller, D. E. L-764406 is a partial agonist of human peroxisome proliferator-activated receptor γ. The role of Cys^{313} in ligand binding. *J. Biol. Chem.* **1999**, *274*, 7913−7922.
(52) Berger, J. P.; Petro, A. E.; Macnaul, K. L.; Kelly, L. J.; Zhang, B. B.; Richards, K.; Elbrecht, A.; Johnson, B. A.; Zhou, G.; Doebber, T. W.; Biswas, C.; Parikh, M.; Sharma, N.; Tanen, M. R.; Thompson, G. M.; Ventre, J.; Adams, A. D.; Mosley, R.; Surwit, R. S.; Moller, D. E. Distinct properties and advantages of a novel peroxisome proliferator-activated protein gamma selective modulator. *Mol. Endocrinol.* **2003**, *17*, 662−676.
(53) Misra, P.; Chakrabarti, R.; Vikramadithyan, R. K.; Bolusu, G.; Juluri, S.; Hiriyan, J.; Gershome, C.; Rajjak, A.; Kashireddy, P.; Yu, S.; Surapureddi, S.; Qi, C.; Zhu, Y. J.; Rao, M. S.; Reddy, J. K.; Ramanujam, R. PAT5A: a partial agonist of peroxisome proliferator-activated receptor gamma is a potent antidiabetic thiazolidinedione yet weakly adipogenic. *J. Pharmacol. Exp. Ther.* **2003**, *306*, 763−771.
(54) Reginato, M. J.; Bailey, S. T.; Krakow, S. L.; Minami, C.; Ishii, C.; Tanaka, H.; Lazar, M. A. A potent antidiabetic thiazolidinedione with unique peroxisome proliferator-activated receptor γ-activating properties. *J. Biol. Chem.* **1998**, *273*, 32679−32684.
(55) Kurosaki, E.; Nakano, R.; Shimaya, A.; Yoshida, S.; Ida, M.; Suzuki, T.; Shibasaki, M.; Shikama, H. Differential effects of YM440 a hypoglycemic agent on binding to a peroxisome proliferator-activated receptor γ and its transactivation. *Biochem. Pharmacol.* **2003**, *65*, 795−805.
(56) Acton, J. J., III; Black, R. M.; Jones, B.; Moller, D. E.; Colwell, L.; Doebber, T. W.; MacNaul, K. L.; Berger, J.; Wood, H. B. Benzoyl 2-methyl indoles as selective PPARγ modulators. *Bioorg. Med. Chem. Lett.* **2005**, *15*, 357−362.
(57) Raspe, E.; Madsen, L.; Lefebvre, A.-M.; Leitersdorf, I.; Gelman, L.; Peinado-Onsurbe, J.; Dallongeville, J.; Fruchart, J.-C.; Berge, R.; Staels, B. Modulation of rat liver apolipoprotein gene expression and serum lipid levels by tetradecylthioacetic acid (TTA) via PPARα activation. *J. Lipid Res.* **1999**, *40*, 2099−2110.
(58) Crestani, M.; Stroup, D.; Chiang, J. Y. L. Hormonal regulation of the cholesterol 7α-hydroxylase gene (*CYP7*). *J. Lipid Res.* **1995**, *36*, 2419−2432.
(59) Hollons, T.; Yoshimura, F. K. Variation in enzymatic transient gene expression assays. *Anal. Biochem.* **1989**, *182*, 411−418.
(60) Rubin, C. S.; Hirsch, A.; Fung, C.; Rosen, O. M. Development of hormone receptors and hormonal responsiveness in vitro. Insulin receptors and insulin sensitivity in the preadipocyte and adipocyte forms of 3T3-L1 cells. *J. Biol. Chem.* **1978**, *253*, 7570−7578.
(61) Vinter, J. G.; Davis, A.; Saunders: M. R. Strategic approaches to drug design. 1. An integrated software framework for molecular modeling. *J. Comput.-Aided Mol. Des.* **1987**, *1*, 31−55.
(62) Weiner, S. J.; Kollman, P. A.; Case, D. A.; Singh, U. C.; Ghio, C.; Alagona, G.; Profeta, S., Jr.; Weiner, P. A new force field for molecular mechanical simulation of nucleic acids and proteins. *J. Am. Chem. Soc.* **1984**, *106*, 765−784. Details of the implementation are given in *Sybyl 6.5 Theory Manual*, Tripos, St. Louis, MO, 1998, p 441.
(63) Gasteiger, J.; Marsili, M. Iterative partial equilization of orbital electronegativity − A rapid access to atomic charges. *Tetrahedron* **1980**, *36*, 3219−3228.
(64) Hagler, A. F.; Lifson, S.; Dauber, P. Consistent force field studies of intermolecular forces in hydrogen-bonded crystals. *J. Am. Chem. Soc.* **1979**, *101*, 5122−5130.

JM0502844